Room-Temperature Dynamics of Vanishing Copper Nanoparticles Supported on Silica

Dohyung Kim,[†,∥] Nigel Becknell,[‡] Yi Yu,[‡] and Peidong Yang*[,†,‡,§,∥]

†Department of Materials Science and Engineering and ‡Department of Chemistry, University of California, Berkeley, California 94720, United States
§Chemical Sciences Division, Lawrence Berkeley National Laboratory, Berkeley, California 94720, United States
∥Kavli Energy Nanosciences Institute, Berkeley, California 94720, United States

S Supporting Information

ABSTRACT: In heterogeneous catalysis, a nanoparticle (NP) system has immediate chemical surroundings with which its interaction needs to be considered, as nanoparticles are typically loaded onto certain supports. Beyond what is known about these interactions, dynamic atomic interactions between the nanoparticle and support could result from the increased energetics at the nanoscale. Here, we show that the dynamic response of atoms in copper nanoparticles to the underlying silica support at room temperature and ambient atmosphere results in the complete disappearance of supported nanoparticles over the course of only a few weeks. A quantitative study of copper nanoparticles at various size regimes (6−17 nm) revealed the significance of size-dependent nanoparticle energetics to the interaction with the support. Extended X-ray absorption fine structure is used to show that copper atoms could readily diffuse into the support to be locally surrounded by oxygen and silicon with structurally disordered outer coordination shells. Increased energetic states at the nanoscale and the energetically favorable configuration of individual copper atoms within silica, identified through EXAFS, are suggested as the cause of nanoparticle disappearance. This unexpected observation opens up new questions as to how nanoparticles interact with surrounding environments that could fundamentally change our conventional view of supported nanoparticle systems.

KEYWORDS: Copper nanoparticles, silica, nanoparticle-support interaction, nanoparticle dynamics
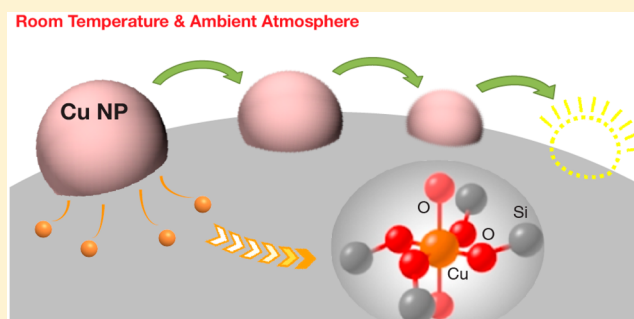
Supported metal and metal oxide nanoparticles are the basis of heterogeneous catalysis, where a wide range of essential processes, such as fuel/chemical production and pollutant mitigation, are conducted.[1−3] The use of nanoparticles requires high surface area oxide supports to finely disperse them to take advantage of their nanoscale dimensions. However, it has also been suggested that supports can play a more active role in dictating catalytic properties of a nanoparticle system by creating a functional interface.[4−7] For instance, the catalytically active sites could be mainly located at the interface between the nanoparticle and support, where both participate at the junction to favorably bind the reactants and intermediates for catalytic conversion.[4,5,7] Furthermore, supports can strongly anchor nanoparticles to resist sintering[6] and catalytic behavior can also be tuned by charge transfer between nanoparticle and support.[8] Therefore, both the nanoparticle and support need to be considered together to evaluate the state and properties of the system for its primary function.

However, beyond the commonly perceived static view of supported nanoparticle systems, dynamic atomic interactions between the nanoparticle and support that could result from the increased energetics at the nanoscale[9−11] need to be considered. The interactions within a supported nanoparticle system could be significant enough to drastically change the state of the system from what was expected.[12−14] Because nanoscale matter possesses far different energetics from its bulk counterpart, the atomic interactions between the nanoparticle and support may take place even under ambient conditions as well. Understanding these interactions will be critical in identifying new types of materials and solving unresolved issues at a more fundamental level that will allow nanomaterials to reach their utmost potential in the relevant fields.

In this work, we have studied the dynamic behavior of copper nanoparticles, utilized for a variety of catalytic reactions including synthesis of methanol and glycol[15,16] and oxidation of volatile organic compounds,[17,18] on silica, a well-known support for nanoparticle loading, under ambient conditions. This study identifies for the first time the dynamic interaction between nanoparticle and support at room temperature, which led to a surprising discovery: complete disappearance of the silica-supported copper nanoparticles under ambient conditions.
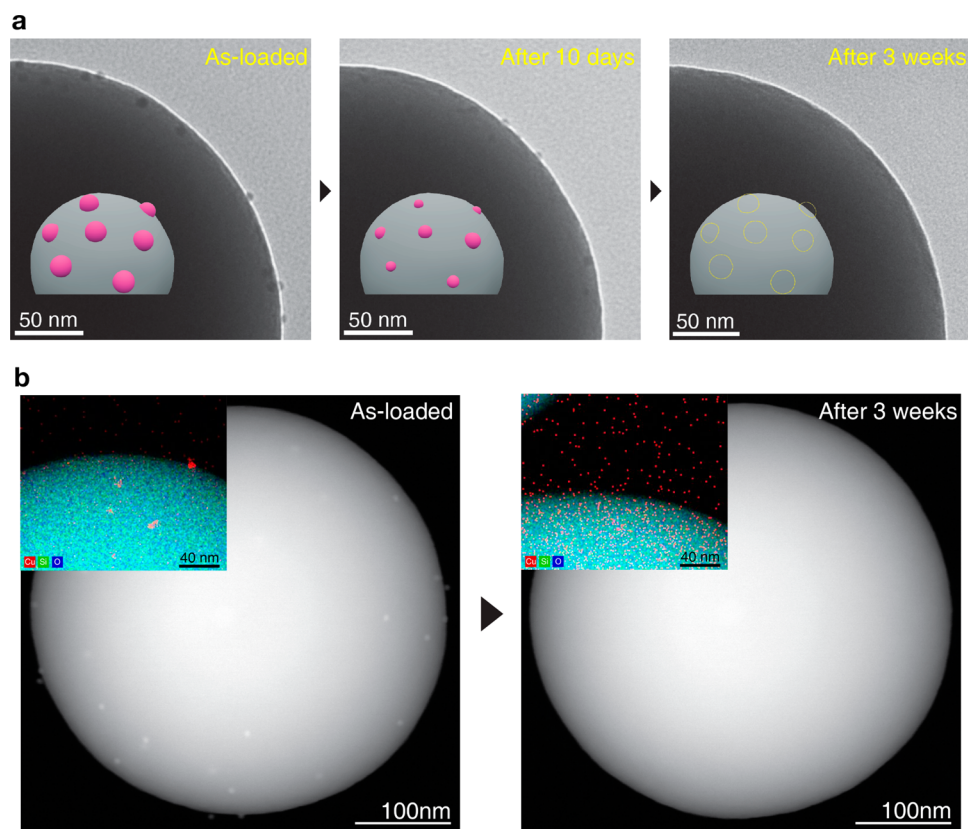
Figure 1. Vanishing of copper nanoparticles on silica. (a) Transmission electron microscopy images of copper nanoparticles (with sizes from 6 to 7 nm) shrinking and disappearing within 3 weeks at room temperature and ambient atmosphere, when supported on amorphous silica. (b) Scanning transmission electron microscopy images of Cu nanoparticles on silica spheres and 3 weeks after loading, where initially loaded particles disappeared. Insets are elemental maps showing Cu (red), Si (green), and O (blue).

The vanishing of copper nanoparticles was accidentally discovered when we attempted to load ligand-removed copper nanoparticles (Figure S1) onto uniform, amorphous silica submicrospheres (loading amount 0.74 mg_{Cu}/g_{Silica}). The shrinkage and ultimate disappearance of Cu nanoparticles (6−7 nm) was observed at room temperature and ambient atmosphere. Ten days after the nanoparticles were initially loaded, only small traces of them could be observed using transmission electron microscopy (TEM) (Figure 1a and Figure S2). Three weeks after loading, Cu nanoparticles could no longer be found. High-angle annular dark field scanning transmission electron microscopy (HAADF-STEM) images of as-loaded Cu nanoparticles on silica (Figure 1b) showed bright intensity originating from Cu nanoparticles over a less-intense background of a silica sphere. However, the bright signal from the nanoparticles was no longer there after 3 weeks and aberration-corrected HAADF-STEM confirmed the complete loss of the nanoparticles (Figure S3). The phenomenon of vanishing Cu nanoparticles was further supported by elemental mapping as shown in the insets of Figure 1b. With increased loadings of Cu nanoparticles on silica, a similar trend was observed as well (Figure S4). In addition, elemental analysis of Cu before and after NP disappearance (details provided in SI) confirmed that the amount of Cu on silica has not changed throughout the process. All of this evidence implied that somehow the copper nanoparticles disappeared on the support at room temperature in ambient conditions, possibly by the migration of Cu atoms constituting each particle into the underlying support. This observation of spontaneous loss of copper nanoparticles on silica is quite surprising as it is very much against conventional wisdom, considering the many previous efforts to construct supported nanoparticle systems for heterogeneous catalysis.

In order to quantitatively understand this unexpected phenomenon, Cu nanoparticles were loaded onto amorphous silicon monoxide support grids in a well dispersed manner, allowing for quantitative tracking of the size of individual particles using TEM. The as-synthesized nanoparticles were loaded on the support grid (Figure 2a and Figure S5) and the grid was heated at 300 °C in air to remove the surface ligands and allow direct contact with the underlying silica support. As expected, the naked copper nanoparticles are typically oxidized partially or completely into Cu_2O upon surface ligand removal (Figure S6). The projected area (in nm^2) of the nanoparticles, assuming a spherical shape, was measured and tracked (Figure 2b and Figure S7) to estimate their size change. Interestingly, we found that the nanoparticles shrank rapidly within a 2 week time period under ambient conditions as shown in Figure 2a. For the case of 8 nm particles, a size decrease of ∼1.5 nm was observed (Figure 2b). In contrast, the particles that were not heat treated (i.e., with surface ligands attached and not in contact with the underlying support) maintained their shapes and actually slightly increased in their size, due to spontaneous oxidation of the metallic copper phase (Figure S8).

We hypothesized that this phenomenon of vanishing Cu nanoparticles could be related to the size-dependent energetics of nanoparticles. Cu nanoparticles with average sizes ranging from 6 to 17 nm (Figure 2a and Figure S9) were tracked in the
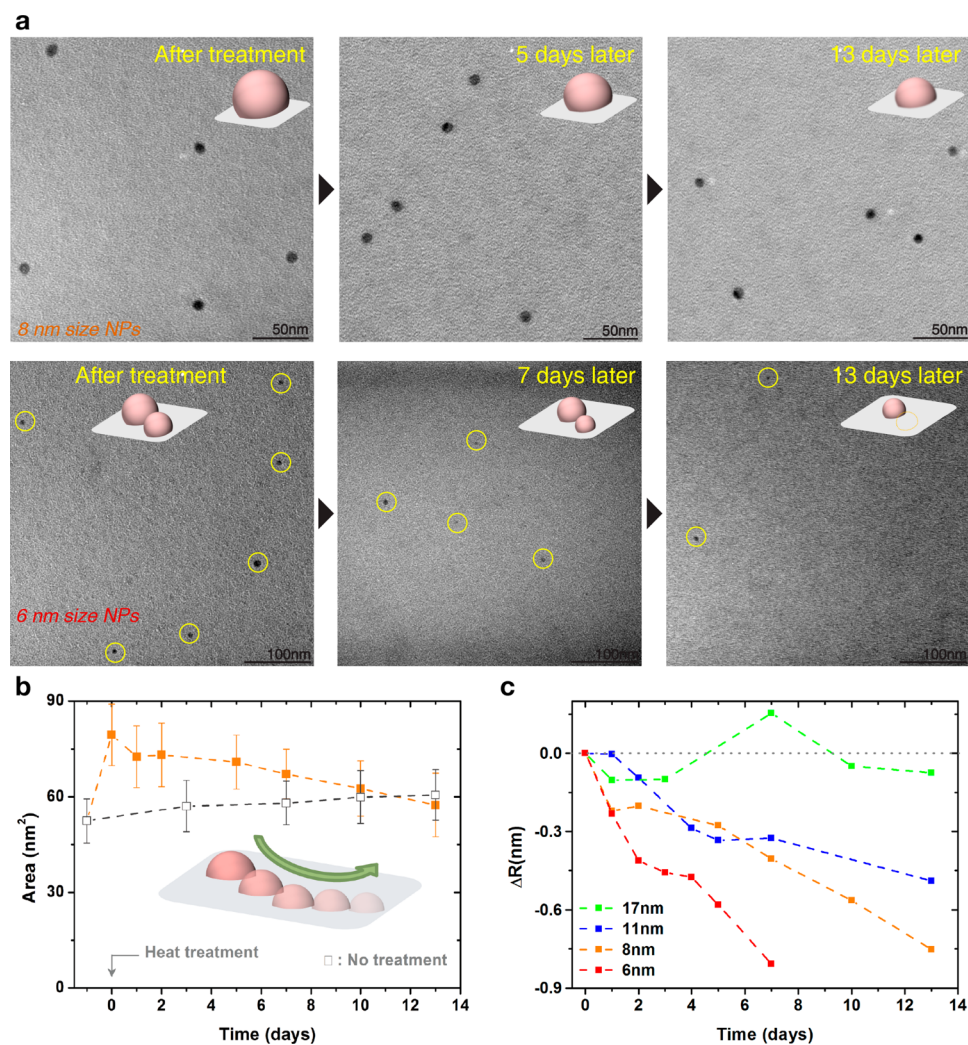
Figure 2. Quantitative analysis of vanishing copper nanoparticles. (a) TEM images showing copper nanoparticles shrinking and disappearing within the 2 week time period on an amorphous silicon monoxide support grid. Smaller particles are highlighted with yellow circles for clarity. (b) Average size, as presented by the projected area (nm^2), of the copper nanoparticles (8 nm) tracked within the 2 week time period after surface ligand removal (closed squares). In comparison, nanoparticles that have not been heat treated (i.e., with the surface ligands remaining) are shown with open squares. Error bars represent one standard deviation. (c) Change in the radius (nm) of copper nanoparticles (average size ranging from 6 to 17 nm) over time on the support grid. The size distribution of 11 nm particles became bimodal due to the initially wide distribution after heat treatment (Figure S13) and the change in radius was calculated from the major component showing the time evolution of the larger particles.

same manner with the ligands removed, allowing direct contact with an oxide support that led to all the particles being partially or completely oxidized.[1] However, the behavior was quite different for the largest particle in that a size decrease was not observed during the same time period (Figure S10). Plotting the change in radius against time for all the particles (Figure 2c and Figure S11) demonstrated a clear trend where the smaller particles declined in size more rapidly. The estimated radial decrease rates are ~0.12, ~0.06, and ~0.04 nm per day for 6, 8, and 11 nm-sized particles, respectively. In other words, the smaller particles exhibited a faster rate of diffusion of the copper atoms into the underlying silica support. For the 6 nm particles, the majority of them disappeared after 2 weeks (Figure 2a). This particle disappearance was measured by tracking the decreasing particle density (number of particles per micron square) over time (Figure S12). The quantitative analysis of how particles of various size regimes evolve revealed not only the possible trigger of this phenomenon, which is the increased energetic state at the nanoscale but also the effect of size-

dependent energetics of nanoscale matter on the rate of the dynamic response of the constituent atoms to the support. Size-dependent energetics of nanoparticles and their constituent atoms are key elements explaining various properties of supported nanoparticles for catalytic applications.[9,19−21] For example, recently, nanoparticle size-dependent chemical potential of Cu atoms on CeO_2 has been reported[10] and control of nanoparticle sintering at high temperature has been demonstrated.[11,22] Importantly, the current observation reveals interesting aspects of nanoparticle thermodynamics even at ambient conditions.

Having observed that the copper nanoparticles can disappear on silica support under ambient conditions, it is important to find out the nature of the copper sites within the silica. X-ray absorption spectroscopy (XAS) was used to specifically probe the copper K-edge of the Cu nanoparticles loaded onto silica spheres, where atomic level information could be obtained in order to elucidate the underlying process of the phenomenon observed. Figure 3a presents extended X-ray absorption fine
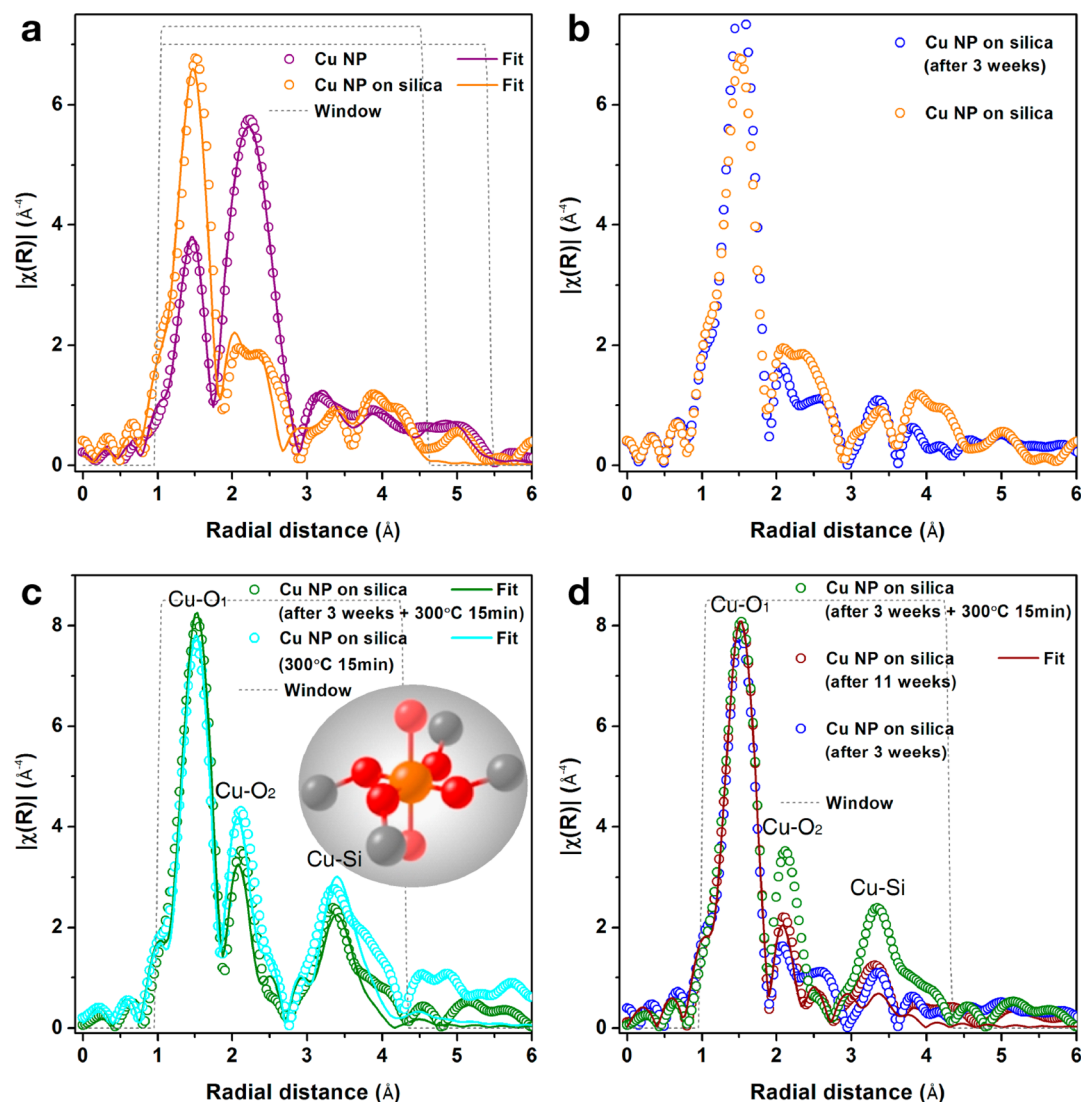
Figure 3. XAS study of vanishing copper nanoparticles on silica support. EXAFS spectra at the Cu K edge comparing Cu nanoparticles as loaded on silica spheres to as-synthesized nanoparticles (a) and 3 weeks after loading (b) in which Cu nanoparticles have completely disappeared. (c) The 3 weeks after and the as-loaded samples were thermally treated under identical conditions and their EXAFS spectra were compared to show the local coordination environment of elemental copper within the matrix. Inset shown is a representation of the coordination environment surrounding Cu identified from the fit with Cu (orange), O_1 (dark red), O_2 (light red), and Si (gray). (d) EXAFS of Cu nanoparticles which were given 11 weeks on silica spheres at room temperature.

structure (EXAFS) data from the Cu nanoparticle itself and after being loaded onto silica spheres. Cu nanoparticles exhibit their strongest feature at 2.2 Å corresponding to nearest Cu neighbors of Cu FCC metal at a bond distance around 2.52 Å. The second strongest peak, below 2 Å, is from the nearest oxygen scattering atoms, indicating that these nanoparticles contain native oxide layers due to the tendency of copper to oxidize. The fit was generated from multiple shells of pure Cu and Cu_2O models (Table S1) and the X-ray absorption near-edge structure (XANES) spectra (Figure S14) also revealed that the as-made particles contained both phases. Cu nanoparticles were further oxidized while loading onto silica spheres as evidenced by the loss of the Cu−Cu interactions and the increase in the first oxygen shell scattering (Figure 3a). Furthermore, the loaded particles had a slightly higher oxidation state compared to Cu_2O nanoparticles (Figures S14 and S15), which may have resulted from direct contact to the relatively oxygen-rich silica support (Figure S16).[1] All of this

indicated that an oxidized copper nanoparticle/silica interface was formed, which is a typical scenario during the preparation of oxide supported copper nanoparticles.

After particle disappearance (after 3 weeks), the EXAFS spectra only displayed a prominent feature for the first oxygen shell (Figure 3b), which increased in amplitude. Any characteristic features of outer shells were very weak and we attribute this to the amorphous nature of the matrix surrounding elemental copper. Cu atoms that migrated away from the original nanoparticle are mainly surrounded by a first shell of oxygen. We hypothesized that there might be an energetically favorable coordination environment for copper within the silica matrix, and the observed disordered structure around copper (Figure 3b) may very well be a kinetically limited transient state before reaching its final configuration. In order to probe whether the coordination environment for Cu atoms would continue to evolve beyond the state we observed after 3 weeks, the 3 weeks old samples were heat treated (300 °C for 15 min)

to accelerate such a transition. The EXAFS spectra (Figure 3c) clearly presented a local structure that extended to at least three shells around copper, where the first two shells (with radial distances of 1.5 and 2.1 Å, respectively) were identified as oxygen at different bond distances and the third shell at 3.4 Å as silicon (Table S2 and inset of Figure 3c). Attributing the first three shells around the Cu absorber to other possible combinations of the elements besides the model used here did not provide a successful fit (see SI methods and Table S3). Furthermore, when the Cu nanoparticles were heat treated under the same conditions but directly after loading onto silica spheres, we found the coordination environment around elemental copper to exhibit the same features (Figure 3c). This indicated that when given enough energy input, copper atoms were being structured to their energetically favorable state within silica. This also meant that copper atoms should eventually reach this final state, though it may be far slower under ambient conditions. Indeed, EXAFS spectra taken after 11 weeks also exhibited the three peaks at the position of the two oxygen shells and the third silicon shell (Figure 3d). When fitted to the model structure, however, the coordination number of the second oxygen shell was only around one (Table S2) most likely due to the fact that copper atoms have not fully transitioned to the final state. This was evident when fitting the third shell, where the Debye−Waller factor was relatively large ($\sigma^2 \sim 0.04$) due to the still amorphous nature of the surrounding elements.[23]

Among the various potential causes of the phenomenon observed (as further discussed in SI), it is possible that the Cu atoms are stabilized by impurities present in silica, considering the low loading conditions of Cu NPs (0.74 mg_{Cu}/g_{Silica}) and the limitation of EXAFS in distinguishing elements of similar atomic number. Therefore, while there is a possibility that the nearest neighbors surrounding Cu may not be purely oxygen, we emphasize that our prediction of the model structure is reasonable, based on previous studies that have identified oxygen-based octahedron motifs for metal ions (including Cu) in silica glass and silicate minerals.[24−28] Another possibility is that the energetically favorable configuration of Cu identified in this work may be induced by naturally present defects in silica, as these sites have been considered to be responsible for metal atom diffusion within the matrix.[29,30] Furthermore, entropic and enthalpic contributions to the change in total free energy have been considered together (details provided in SI). From this view, it is important to note that the increased energetics associated with decreasing size of the nanoparticles could facilitate Cu atoms to energetically favor the identified local configuration of Cu within the silica matrix.

We have also conducted initial simulations of the Cu-silica system for the phenomenon observed using molecular dynamics. More specifically, amorphous SiO_2 was obtained using the melt-quench technique[31] and ReaxFF potentials[32] and the final structure was then further relaxed with density functional theory[33] calculations. However, due to its inherently complex and ill-defined nature, amorphous silica structures with identical Si−O composition can have slightly varying energy levels, subject to both the long-range and short-range disorders. The large degree of freedom in this system (including the previously mentioned factors possibly contributing to the energetic stability of Cu in the local coordination environment identified in this work) makes thermodynamic assessment of Cu diffusion from a nanoparticle into silica challenging and error-prone, and assessing the kinetics of this process is

certainly not feasible at this time. However, from the EXAFS study, we could show that the supported copper nanoparticles vanished into the silica support by the dynamic movement of copper atoms, eventually stabilizing in a coordination environment surrounded by shells of oxygen and silicon atoms. Together with the quantitative study of the phenomenon, we can conclude that the driving force for copper atom diffusion into silica is the favorable local configuration within the matrix identified through EXAFS in comparison to the relatively high energy state in small nanoparticle form. Also, this leads to the possibility that supported Cu nanoparticles may actually be in a state of nanoparticles together with single atom species within the supporting matrix.

Supported metal nanoparticles have been used for various applications where the supporting substrate is typically used to stably hold the nanoparticles and to create a nanoscale junction.[5−7,22,34] The fact that copper nanoparticles can interact with the underlying amorphous silica support by the movement of copper atoms even under ambient conditions opens up many fundamental questions regarding the nature of supported metal nanoparticles and the resulting chemical and physical properties.[35−37] For example, the observed catalytic activities of supported copper nanocatalysts may not be from the particles alone, but in addition or even alternatively the copper sites located within the matrix could in principle contribute synergistically.[15,38,39]

■ ASSOCIATED CONTENT

Ⓢ Supporting Information

The Supporting Information is available free of charge on the ACS Publications website at DOI: 10.1021/acs.nanolett.7b00942.

> Experimental details and additional characterization data. (PDF)

■ AUTHOR INFORMATION

Corresponding Author

*E-mail: p_yang@berkeley.edu.

ORCID ⊙

Peidong Yang: 0000-0003-4799-1684

Author Contributions

D.K. and P.Y. designed the experiments and wrote the paper. D.K. performed the experiments. N.B. performed XAS experiments and analyzed the data. Y.Y. carried out HRTEM imaging and elemental analysis. All authors discussed the results and commented on the manuscript.

Notes

The authors declare no competing financial interest.

■ ACKNOWLEDGMENTS

■ REFERENCES

(1) Bell, A. T. *Science* **2003**, *299* (5613), 1688−1691.

(2) Wang, S.; Wang, Z.; Zha, Z. *Dalt. Trans* **2009**, No. 43, 9363−9373.

(3) White, R.; Luque, R.; Budarin, V.; Clark, J.; Macquarrie, D. *Chem. Soc. Rev.* **2009**, *38* (2), 481−494.

(4) Fu, Q.; Li, W. X.; Yao, Y.; Liu, H.; Su, H. Y.; Ma, D.; Gu, X. K.; Chen, L.; Wang, Z.; Zhang, H.; Wang, B.; Bao, X. *Science* **2010**, *328* (5982), 1141−1144.

(5) Cargnello, M.; Doan-Nguyen, V. V. T.; Gordon, T. R.; Diaz, R. E.; Stach, E. A.; Gorte, R. J.; Fornasiero, P.; Murray, C. B. *Science* **2013**, *341* (6147), 771−773.

(6) Farmer, J. A.; Campbell, C. T. *Science* **2010**, *329* (5994), 933−936.

(7) Comotti, M.; Li, W. C.; Spliethoff, B.; Schüth, F. *J. Am. Chem. Soc.* **2006**, *128* (3), 917−924.

(8) Schwab, G. M. *Adv. Catal.* **1979**, *27*, 1−22.

(9) Campbell, C. T.; Sellers, J. R. V. *Faraday Discuss.* **2013**, *162*, 9.

(10) James, T. E.; Hemmingson, S. L.; Campbell, C. T. *ACS Catal.* **2015**, *5* (10), 5673−5678.

(11) Campbell, C. T.; Parker, S. C.; Starr, D. E. *Science* **2002**, *298* (5594), 811−814.

(12) Ajayan, P. M.; Marks, L. D. *Nature* **1989**, *338* (6211), 139−141.

(13) Gal, P. L.; Smith, B. C.; Owen, G. *Nature* **1990**, *348* (6300), 430−432.

(14) Liu, J. J. *ChemCatChem* **2011**, *3* (6), 934−948.

(15) Wang, Z. Q.; Xu, Z. N.; Peng, S. Y.; Zhang, M. J.; Lu, G.; Chen, Q. S.; Chen, Y.; Guo, G. C. *ACS Catal.* **2015**, *5* (7), 4255−4259.

(16) Liu, H.; Huang, Z.; Xia, C.; Jia, Y.; Chen, J.; Liu, H. *ChemCatChem* **2014**, *6* (10), 2918−2928.

(17) Larsson, P. O.; Andersson, A. *J. Catal.* **1998**, *179* (1), 72−89.

(18) Huo, C.; Ouyang, J.; Yang, H. *Sci. Rep.* **2014**, *4*, 3682.

(19) Xu, X.; He, J.; Goodman, D. W. *J. Chem. Phys.* **1993**, *284*, 103−108.

(20) Duriez, C.; Henry, C. R.; Chapon, C. *Surf. Sci.* **1991**, *253* (1−3), 190−204.

(21) Henry, C. R. *Surf. Sci. Rep.* **1998**, *31*, 231−325.

(22) Wettergren, K.; Schweinberger, F. F.; Deiana, D.; Ridge, C. J.; Crampton, A. S.; Rötzer, M. D.; Hansen, T. W.; Zhdanov, V. P.; Heiz, U.; Langhammer, C. *Nano Lett.* **2014**, *14* (10), 5803−5809.

(23) Johnson, S. L.; Heimann, P. A.; Lindenberg, A. M.; Jeschke, H. O.; Garcia, M. E.; Chang, Z.; Lee, R. W.; Rehr, J. J.; Falcone, R. W. *Phys. Rev. Lett.* **2003**, *91* (15), 157403.

(24) Fukumi, K.; Chayahara, A.; Kadono, K.; Kageyama, H.; Akai, T.; Mizoguchi, H.; Kitamura, N.; Makihara, M.; Horino, Y.; Fujii, K. *J. Mater. Res.* **2001**, *16* (1), 155−162.

(25) Maurizio, C.; D'Acapito, F.; Benfatto, M.; Mobilio, S.; Cattaruzza, E.; Gonella, F. *Eur. Phys. J. B* **2000**, *14* (2), 211−216.

(26) Evans, H. T.; Mrose, M. E. *Am. Mineral.* **1977**, *62*, 491−502.

(27) Toupance, T.; Kermarec, M.; Lambert, J.-F.; Louis, C. *J. Phys. Chem. B* **2002**, *106* (9), 2277−2286.

(28) Farges, F.; Benzerara, K.; Brown, G. E. In *AIP Conference Proceedings*; AIP, 2007; Vol. *882*, pp 223−225.

(29) Min, B. K.; Santra, A. K.; Goodman, D. W. *J. Vac. Sci. Technol., B: Microelectron. Process. Phenom.* **2003**, *21* (6), 2319−2323.

(30) van den Oetelaar, L. C. A.; Partridge, A.; Toussaint, S. L. G.; Flipse, C. F. J.; Brongersma, H. H. *J. Phys. Chem. B* **1998**, *102*, 9541−9549.

(31) Pham, H. H.; Wang, L.-W. *Phys. Chem. Chem. Phys.* **2015**, *17*, 11908−11913.

(32) van Duin, A. C. T.; Strachan, A.; Stewman, S.; Zhang, Q.; Xu, X.; Goddard, W. A., III *J. Phys. Chem. A* **2003**, *107* (19), 3803−3811.

(33) Kohn, W.; Sham, L. J. *Phys. Rev.* **1965**, *140* (4A), A1133.

(34) Zheng, N.; Stucky, G. D. *J. Am. Chem. Soc.* **2006**, *128* (44), 14278−14280.

(35) Liu, P.; Zhao, Y.; Qin, R.; Mo, S.; Chen, G.; Gu, L.; Chevrier, D. M.; Zhang, P.; Guo, Q.; Zang, D.; Wu, B.; Fu, G.; Zheng, N. *Science* **2016**, *352* (6287), 797−800.

(36) Guo, X.; Fang, G.; Li, G.; Ma, H.; Fan, H.; Yu, L.; Ma, C.; Wu, X.; Deng, D.; Wei, M.; Tan, D.; Si, R.; Zhang, S.; Li, J.; Sun, L.; Tang, Z.; Pan, X.; Bao, X. *Science* **2014**, *344* (6184), 616−619.

(37) Nolte, P.; Stierle, A.; Jin-Phillipp, N. Y.; Kasper, N.; Schulli, T. U.; Dosch, H. *Science* **2008**, *321* (5896), 1654−1658.

(38) Chen, L. F.; Guo, P. J.; Qiao, M. H.; Yan, S. R.; Li, H. X.; Shen, W.; Xu, H. L.; Fan, K. N. *J. Catal.* **2008**, *257* (1), 172−180.

(39) Gong, J.; Yue, H.; Zhao, Y.; Zhao, S.; Zhao, L.; Lv, J.; Wang, S.; Ma, X. *J. Am. Chem. Soc.* **2012**, *134* (34), 13922−13925.